Determining Spin-Lattice Relaxation Times and Gyromagnetic Ratios Using Nuclear Magnetic Resonance

The Ohio State University, Department of Physics, Columbus, OH 43210

Colin Voorhis
Partners: Emily Macbeth, Hirak Basu

April 1st, 2025

Abstract

This experiment analyzes nuclear magnetic resonance (NMR), a physical phenomenon where particles with magnetic moments precess about external magnetic fields at a frequency dependent on the particle's composition and the strength of the field. In this experiment, particles are made to precess about Earth's magnetic field, and a voltage signal is extracted from the resulting precession. The spin-lattice relaxation time of the proton and the gyromagnetic ratios of multiple particles are found to within 30% of their accepted values. The form of the Curie law is also verified.

1 Introduction

Elementary particles such as protons and neutrons have magnetic moments generated by their spin angular momentum and internal structure. These magnetic moments will precess around an external magnetic field if placed within one. This phenomenon is known as Larmor precession, and can be used to derive information about the particles undergoing precession. The field of nuclear magnetic resonance, for example, uses Larmor precession to study the composition of organic materials, the molecular structure of catalysts, and certain properties of elementary particles [1].

In this experiment, Earth's magnetic field is used as an external magnetic field to induce Larmor precession. We aim to determine the spin-lattice relaxation time for the proton, which describes the rate at which magnitude moments in a sample align with an external magnetic field. We also aim to verify the form of the Curie Law, which relates the alignment of magnetic moments within a sample to the magnitude of the external magnetic field that causes the alignment. Finally, we aim to determine the gyromagnetic ratio of the proton and fluorine, which relates a particle's magnetic moment to its spin angular momentum.

2 Theory

2.1 Magnetization

Protons and neutrons have $\vec{\mu}$ which arise from their inherent spin angular momentum and quark composition. Atomic nuclei can also have $\vec{\mu}$ when they contain unpaired protons and neutrons; paired protons and paired neutrons generally cancel each other's $\vec{\mu}$ due to their opposed spins. See Appendix A.1 for further discussion of this phenomenon. For these systems, $\vec{\mu}$ is proportional to the spin angular momentum $\vec{L}$ of the system and a gyromagnetic ratio γ [2]:

$$\vec{\mu} = \gamma \vec{L} \tag{1}$$

For a sample containing many particles, we can define an overarching magnetic moment per unit volume, or magnetization $\vec{M}$. A non-zero $\vec{M}$ can be generated in sample by placing it in an external magnetic field $\vec{B}$. Appendix 2 derives the Curie Law, which relates equilibrium magnetization $\vec{M_0}$ and B [2] [3]:

$$M_0 = \frac{N\mu^2 B}{3k_b T} \tag{2}$$

where:

- k_b is the Boltzmann constant
- T is the temperature of the system

Once a magnetic field is applied to the sample its magnetization will exponentially approach M_0 as its particles align with $\vec{B}$ over time [2]:

$$M(t) = M_0 \left(1 - e^{-t/T_1}\right) \tag{3}$$

T_1 is a characteristic time constant known as the spin-lattice relaxation time, which represents the time a sample takes to reach $M = (1 - e^{-1})M_0$.

If $\vec{B}$ is subsequently terminated, the sample's particles will return to a random distribution of $\vec{\mu}$ directions over time. This process is similarly governed by the spin-spin relaxation time T_2. In practice, T_2 is substantially impacted by the inhomogeneities in $\vec{B}$ and difficult to calculate directly. We instead measure the observed spin-spin relaxation time T_2^*:

$$M(t) = M_0\, e^{-t/T_2^*} \tag{4}$$

2.2 Precession

Particles with $\vec{\mu}$ placed in $\vec{B}$ will not just align with $\vec{B}$ and reach a static equilibrium position, but will instead precess about $\vec{B}$. Per Appendix A.3, the angular frequency ω of this precession is proportional to the magnitude of $\vec{B}$ and γ [4]:

$$\omega = \gamma B \tag{5}$$

The magnetization of a sample of particles will precess in the same manner, since $\vec{M} \propto \vec{\mu}$.

In this experiment, $\vec{M}$ is made to precess about Earth's magnetic field $\vec{B}_\oplus$. This field can be added to using a set of Helmholtz coils, which are described in Appendix A.4. These coils produce a magnetic field proportional to the current I_H passed through them and a proportionality constant k. The recorded precession frequency $f = \omega/2\pi$ can therefore be defined as:

$$f = \frac{\gamma\,(B_\oplus + kI_H)}{2\pi} \tag{6}$$

2.3 EFNMR Apparatus

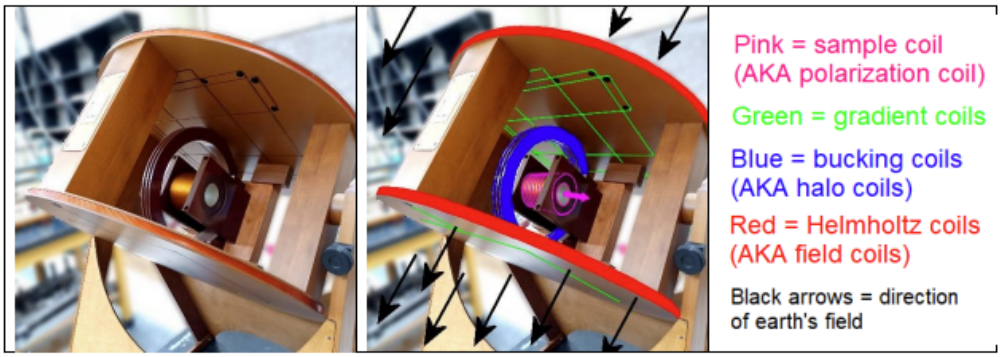

Figure 1: This figure displays the external coils of the EFNMR apparatus with color-coded coils [5].

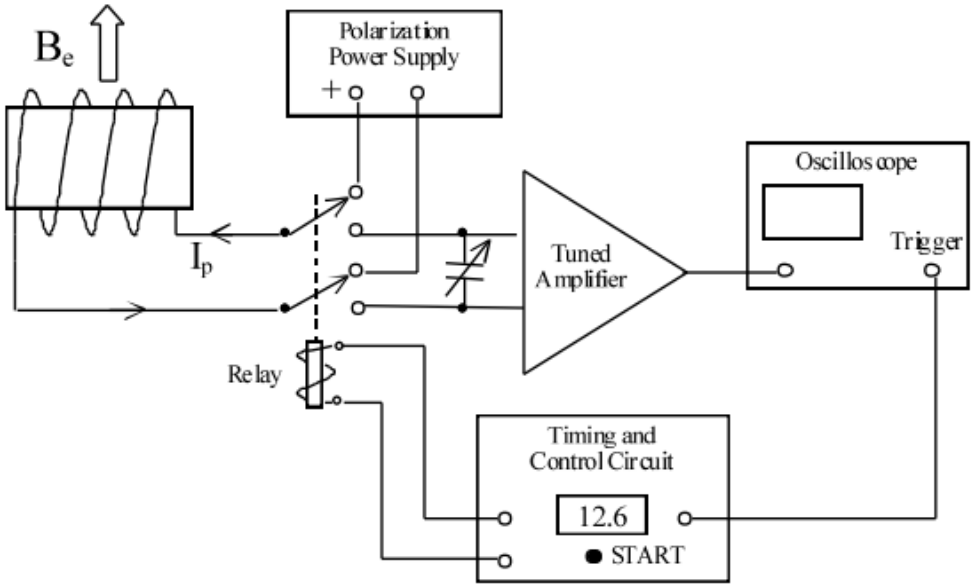

Figure 2: This figure displays a simplified block diagram of the EFNMR apparatus's circuitry [2].

In this experiment, a series of wire coils are used to polarize a liquid sample for a set time and with a specified current, and record the resulting precession using magnetic induction. The EFNMR apparatus coils are shown in Figure 1. Figure 2 displays a simplified block diagram of the circuit that accomplishes this procedure. The apparatus must be aligned such that the plane the Helmholtz coils lie in is perpendicular to $\vec{B}_\oplus$. This will cause the field generated by the Helmholtz coils to add to $\vec{B}_\oplus$.

The apparatus can be tuned to amplify certain frequency ranges in these signals. For best results, the apparatus should be tuned to amplify the signal's frequency of precession as much as possible. See Appendix A.5 for further discussion of this amplification system.

3 Determining Spin-Lattice Relaxation Times

The maximum zero-to-peak voltage V of the free precession signal for a given polarization time t_p is proportional to $\vec{M}(t_p)$ from Eq. 3. A signal from a sample with magnetization M_0 can be achieved by setting $t_p \geq 5T_1$. Lower polarization times will produce signals with lower sample magnetization. A given sample's T_1 can be determined by recording V for a variety of t_p, using V in place of M:

$$V(t_p) = V_0 \left(1 - e^{-t_p/T_1}\right) \tag{7}$$

Figure 3 plots recorded voltages against polarization times, and the parameters of the resulting fits are contained in Table 1. The error on voltage is derived from the oscilloscope, and the error on polarization time is estimated from the display of the apparatus. See Appendix B.1 for further discussion of fitting techniques and uncertainties.

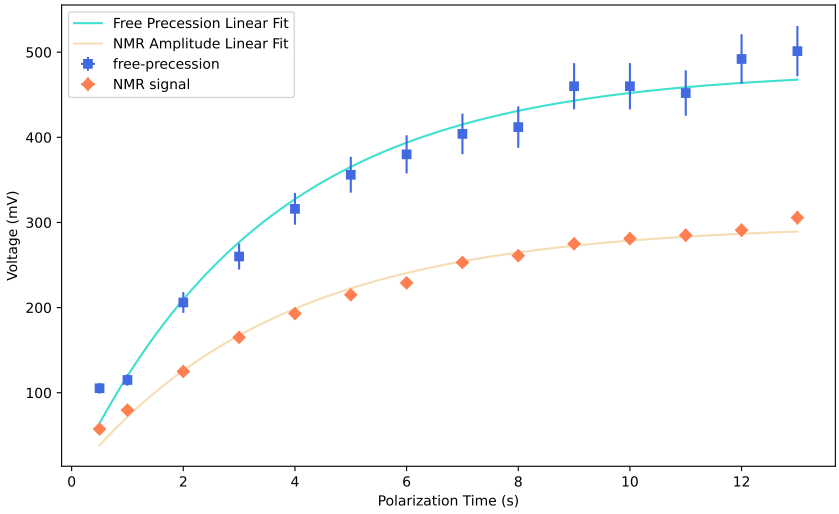

Figure 3: This plot displays the magnetization of a tap water sample as a function of polarization time. The free precession fit has $\chi^2/\text{dof} = 2.41$. The NMR amplitude fit has $\chi^2/\text{dof} = 3.41$. Error bars are present, but small, for both axes.

Parameter Source	V_0 (mV)	T_1 (s)	χ^2/dof
Free Precession Signal	479.1 ± 23.6	3.48 ± 0.38	2.40
NMR Amplitude Signal	297.63 ± 8.36	3.63 ± 0.25	3.41

Table 1: This table displays the fitting parameters of Eq. 7 calculated for both the free precession and NMR amplitude signals.

We estimate an overall spin-lattice relaxation time $T_1 = 3.54 \pm 0.21\,\text{s}$ based on a weighted average of each method's fitted T_1. This is within 30% of the expected $T_1 = 2.5\,\text{s}$ [5]. Differences between the two values are likely due to tuning issues with the apparatus as described in Appendix C.

The χ^2/dof for both fits is close to 1, indicating Eq. 7 does accurately model the behavior of this system. $\chi^2/\text{dof} > 1$ for both fits as well, suggesting uncertainties are underestimated for this data.

The measured spin-spin relaxation time T_2^* is found by fitting the decay of the free precession and NMR amplitude signals to Eq. 4, using V in place of M:

$$V(t_p) = V_0\, e^{-t_p/T_2^*} \tag{8}$$

Our collected data for this measurement was not usable for fitting due to issues with calibrating the gradient field coils of the apparatus. See Appendix C.1 for further information.

4 Verifying the Form of the Curie Law

The current I_s passed through the sample coil will generate a magnetic field with strength B within the coil. Varying I_s will therefore determine the equilibrium magnetization M_0 for the sample per Eq. 2. The Curie law's reliance on B can be verified by recording V for a variety of I_s, using V in place of M_0 and I_s in place of B:

$$V_0 = mI + b \tag{9}$$

In this case, m and b are linear fitting parameters.

Figure 4 plots recorded voltages against polarization currents. The error on voltage is derived from the oscilloscope, and the error on current is derived from the sample coil's power supply. See Appendix B.2 for more information on uncertainty.

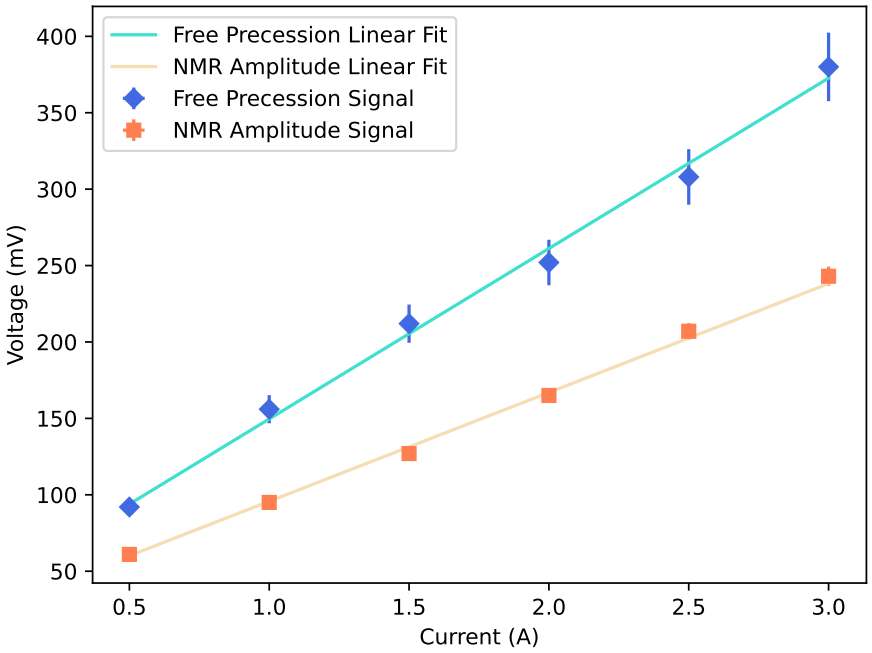

Figure 4: This plot displays the magnetization of a tap water sample as a function of sample coil polarization current. The free precession fit has $\chi^2/\text{dof} = 0.40$. The NMR amplitude fit has $\chi^2/\text{dof} = 0.89$. Error bars are present, but small, for both axes.

$\chi^2/\text{dof} = 0.40$ for the free precession signal, and $\chi^2/\text{dof} = 0.89$ for the NMR amplitude signal. Both values are close to 1, indicating that Eq. 9 does accurately model the behavior of this system. This verifies the form of the Curie law provided in Eq. 2. $\chi^2/\text{dof} < 1$ for both fits as well, suggesting uncertainties are overestimated for this data.

5 Determining Gyromagnetic Ratios

The current I_H passed through the Helmholtz coils will generate a field which adds to $\vec{B}_\Phi$ as described by Eq. 6. Varying I_H will therefore vary the frequency of precession of the sample's magnetization f. The γ of a given sample's particles can be determined by recording f for a variety of I_H:

$$f = mI_H + b \tag{10}$$

where the linear fitting parameters m and b are defined as

$$m = \frac{\gamma k}{2\pi} \qquad b = \frac{\gamma B_\Phi}{2\pi} \tag{11}$$

Figure 5 plots recorded frequencies against Helmholtz coil currents for tap water. Figure 6 plots frequency versus current for a liquid fluorine compound. Table 2 contains the fitting parameters and calculated gyromagnetic ratios for each sample. The error on frequency is derived from the oscilloscope, and the error on current is derived from the multimeter used to measure it. See Appendix B.3 for more information on fitting and uncertainty.

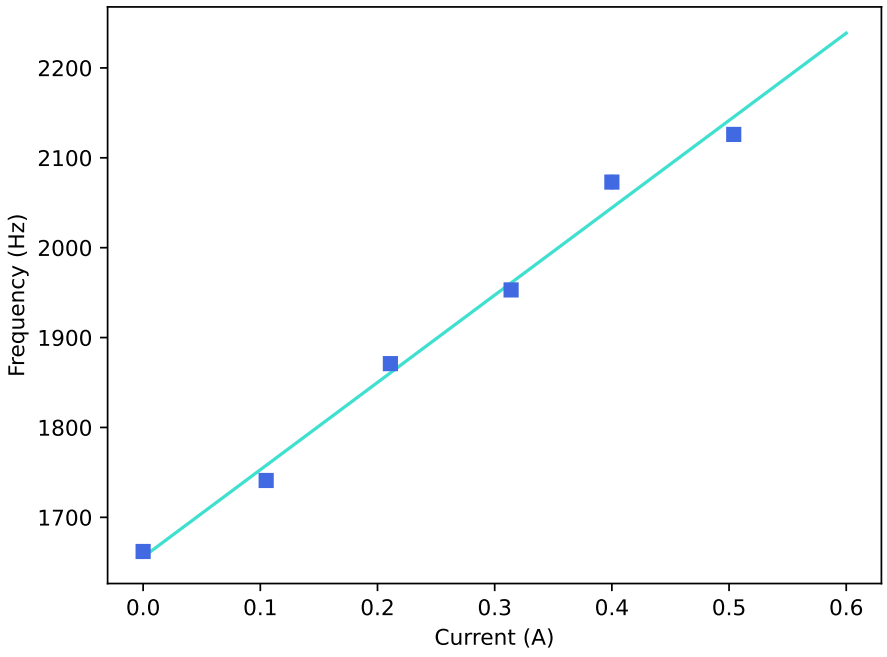

Figure 5: This plot displays the frequency of the Larmor precession of tap water as a function of Helmholtz coil current. The resulting fit has $\chi^2/\text{dof} = 3.88$. Error bars are present, but small, for both axes.

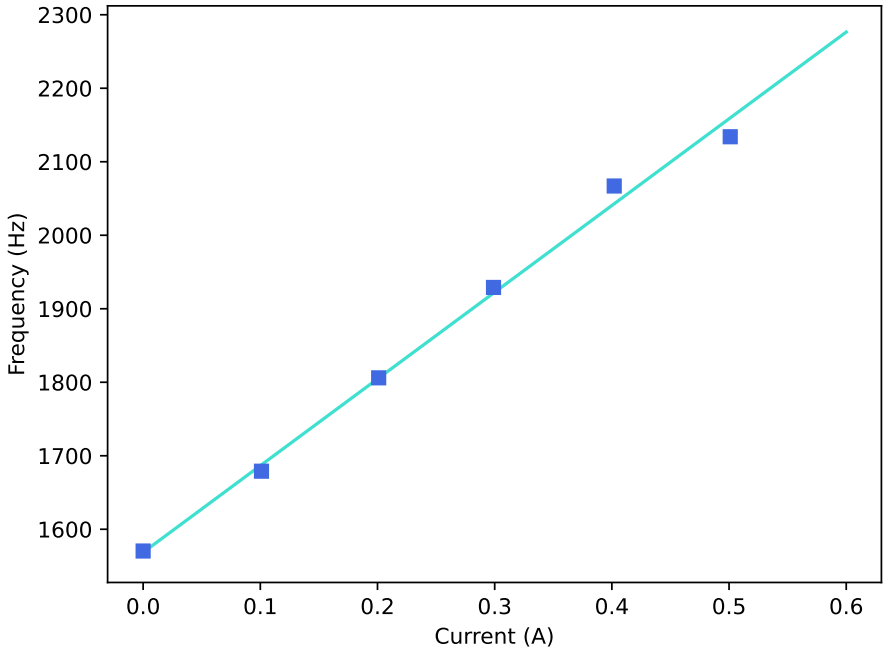

Figure 6: This plot displays the frequency of the Larmor precession of a liquid fluorine compound as a function of Helmholtz coil current. The resulting fit has $\chi^2/\text{dof} = 2.01$. Error bars are present, but small, for both axes.

Sample Composition	m	b	χ^2/dof	γ (rad/s T)	$\lvert$Rel. err$\rvert$
Tap Water	971.6 ± 45.8	1656 ± 12	3.88	$1.882 \pm 0.099 \cdot 10^8$	29.6%
Fluorine	$1180. \pm 38$	$1568 \pm 10.$	2.012	$2.286 \pm 0.090 \cdot 10^8$	20.1%

Table 2: This table displays the fitting parameters of Eq. 10 and calculated gyromagnetic ratios for water and a liquid fluorine compound. It also compares these gyromagnetic ratios to their generally accepted values: $2.675 \cdot 10^8$ rad/s T for protons and $2.517 \cdot 10^8$ rad/s T for fluorine.

We estimate the gyromagnetic ratio of the proton via tap water as $1.882 \pm 0.099 \cdot 10^8$ rad/s T, which is within 30% of its accepted value. We estimate the gyromagnetic ratio of fluorine as $2.012 \pm 0.090 \cdot 10^8$ rad/s T, which is within 20% of its accepted value. Again, discrepancies between estimated values and known values are likely due to issues with tuning the apparatus as described in Appendix C.

The χ^2/dof for both fits is close to 1, indicating Eq. 10 does accurately model the behavior of this system. $\chi^2/\text{dof} > 1$ for both fits as well, suggesting uncertainties are underestimated for this data.

A Supplementary Theory

A.1 Elementary Particle Magnetic Moments

According to Maxwell's equations, any charge distribution moving at a speed $\vec{v}$ relative to a magnetic field $\vec{B}$ will experience a force perpendicular to $\vec{v}$ and $\vec{B}$. Charge distributions can also experience a torque $\vec{\tau}$ due to this effect. If $\vec{B}$ is constant, then a magnetic moment $\vec{\mu}$ can be defined such that

$$\vec{\tau} = \vec{\mu} \times \vec{B} \tag{12}$$

Consider a point particle with mass m and charge q traverses a circular path with radius r at a constant angular velocity ω. The magnitude of $\vec{L}$ can be defined as

$$L = mr^2\omega = mr^2 \cdot 2\pi f \tag{13}$$

where f is the frequency of the particle's rotation.

This particle will also produce an average current $I = qf$ in the loop in travels. Its magnetic moment will point in the same direction as $\vec{L}$, and its magnitude can be defined as follows:

$$\mu = I \cdot \pi r^2 = qf \cdot \pi r^2 = q \cdot \frac{\omega}{2} \cdot r^2 = q \cdot \frac{mr^2\omega}{2m} = \frac{q}{2m} \cdot L \tag{14}$$

In short, the system's magnetic moment and angular momentum are proportional. This is because the rotational motion of the particle is the source of both $\vec{\mu}$ and $\vec{L}$ for this system. Defining a gyromagnetic ratio $\gamma = q/2m$ for this system gives Eq. 1.

Elementary particles such as protons and neutrons follow this same principle. The spin angular momentum of the quarks that make up these particles, which are charged, generates a $\vec{\mu} \propto \vec{L}$ [6]. Note that while their spin angular momentum is an inherent quantum property, rather than caused by a physical rotation, it maintains many of the same properties as the previous physical example. These elementary particles will also have γ that relate their $\vec{\mu}$ and $\vec{L}$, which can be determined experimentally.

Atomic nuclei are composed of one or more protons and neutrons. Pairs of protons and neutrons in an atomic nucleus will posses opposite spin states. This is due to the Pauli exclusion principle: two fermions cannot occupy the same quantum state simultaneously [7]. Paired protons and neutrons will therefore have $\vec{\mu}$ with equal magnitudes and opposite directions, which cancel each other on a macroscopic scale. Therefore, atomic nuclei will only have a net $\vec{\mu}$ if they contain an unpaired proton or neutron.

A.2 Curie Law Derivation

The torque applied to the particles in an external magnetic field $\vec{B}$ tends to align their magnetic moments $\vec{\mu}$ with $\vec{B}$. Two nuclei with opposed $\vec{\mu}$ will cancel each other's magnetization contributions across the full sample, so $\vec{M}$ is proportional to the difference between the number of $\vec{\mu}$ pointing with the field versus against it:

$$M \propto n_{\uparrow}\mu - n_{\downarrow}\mu \tag{15}$$

In this equation:

- M is the magnitude of the magnetization of the sample
- n_{up} is the number of particles pointing the same direction as $\vec{B}$
- n_{down} is the number of particles pointing the opposite direction to $\vec{B}$
- $\vec{\mu}$ is the magnitude of each particle's magnetic moment

This difference in directions of magnetic moments can be quantified. The following derivation is adapted from Chapter 11 of Kittel's Introduction to Solid State Physics [3].

The magnetization M of a system of particles can be defined as

$$M = N\mu\langle\cos(\theta)\rangle \tag{16}$$

where:

- M is the magnetization (magnetic moment per unit volume) of the sample
- N is the number of magnetic moments per unit volume
- μ is the magnitude of an individual magnetic moment
- θ is the angle between $\vec{\mu}$ and $\vec{B}$ for a given particle
- $\langle\cos(\theta)\rangle$ is the average value of $\cos(\theta)$ for all $\vec{\mu}$ in the sample

$\langle\cos(\theta)\rangle$ can be calculated for 2-state particles using the partition function:

$$\langle\cos(\theta)\rangle = \tanh\left(\frac{\mu B}{k_b T}\right) \tag{17}$$

where:

- B is the external magnetic field over the sample
- k_b is the Boltzmann constant
- T is the temperature of the sample

The equilibrium magnetization M_0 for a sample can then be defined as

$$M_0 = \mu N \tanh\left(\frac{\mu B}{k_b T}\right) \tag{18}$$

This equation can be simplified by assuming that $\mu B/k_b T << 1$, which is the case for all samples analyzed in this experiment. In this case $\tanh(x) \approx x$:

$$\tanh\left(\frac{\mu B}{k_b T}\right) \approx \frac{\mu B}{k_b T} \tag{19}$$

and M_0 is approximated as

$$M_0 \approx \frac{N\mu^2 B}{k_b T} \tag{20}$$

If we account for systems with a greater angular momentum quantum numbers, $\langle\cos(\theta)\rangle$ is instead

$$\langle\cos(\theta)\rangle = L\left(\frac{\mu B}{k_b T}\right) \tag{21}$$

where $L(x) = \coth(x) - 1/x$ is the Langevin function. In this case, $L(x) \approx x/3$ when $\mu B/k_b T << 1$:

$$L\left(\frac{\mu B}{k_b T}\right) \approx \frac{\mu B}{3k_b T} \tag{22}$$

giving the classical form of the Curie law shown in Eq. 2.

A.3 Larmor Precession

Consider an elementary particle in an external magnetic field $\vec{B}$. The torque $\vec{\tau}$ on this particle can be defined by combining Eqs. 12 and 1:

$$\vec{\tau} = \gamma\vec{L} \times \vec{B} \tag{23}$$

$\vec{\tau}$ can also be defined as a change in $\vec{L}$ over time:

$$\vec{\tau} = \frac{d\vec{L}}{dt} \tag{24}$$

Combining these two equations gives the following:

$$\frac{d\vec{L}}{dt} = \gamma\vec{L} \times \vec{B} \tag{25}$$

So, $\vec{L}$ is governed by a differential equation. Due the the cross product in this equation, $d\vec{L}/dt$ is always perpendicular to both $\vec{L}$ and $\vec{B}$. Since the magnitudes of $\vec{B}$ and $\vec{L}$ are fixed, only the direction of $\vec{L}$ will change due to $d\vec{L}/dt$. This indicates that $\vec{L}$ will precess around $\vec{B}$. This phenomenon is called Larmor precession. The angular frequency ω of this precession has the same magnitude as the values $\vec{L}$ is multiplied by:

$$\omega = \gamma B \tag{26}$$

A.4 Helmholtz Coil Field

In this experiment, $\vec{B}_\oplus$ can be added to using an additional $\vec{B}$ generated by a set of Helmholtz coils. These coils produce a relatively uniform magnetic field with magnitude [5]

$$B = \left(\frac{4}{5}\right)^{3/2} \cdot \frac{N\mu_0 I}{R} \tag{27}$$

at their center, where:

- B is the magnitude of the field
- $N = 11$ is the number of turns in each coil
- $\mu_0 = 4\pi \cdot 10^{-7}\,\mathrm{T\,m\,A^{-1}}$ is the permeability of free space
- I is the current passed through the coils
- $R = 0.305 \pm 0.005\,\mathrm{m}$ is the radius of the coils

The proportionality constant k in Eq. 6 can therefore be defined as

$$k = \left(\frac{4}{5}\right)^{3/2} \cdot \frac{N\mu_0}{R} \tag{28}$$

A.5 Amplifier

The voltage output by the coil in this experiment can be amplified by a specially designed RLC circuit. For a properly designed, tuned, and resonant circuit with inductance L and resistance R, a quality factor $Q = R/\omega L$ exists such that [4]

$$V_{out} = Q \cdot \mathrm{emf} \tag{29}$$

The TeachSpin apparatus has $Q \approx 80$ [4].

The RLC circuit will not uniformly amplify the output voltage; certain frequencies will be amplifed more than others. Frequencies are amplified most when the circuit's capacitive reactance X_C and inductive reactance X_L are equal. These values can be defined as

$$X_C = \frac{1}{\omega C} \tag{30}$$

$$X_L = \omega L \tag{31}$$

where:

- ω is the desired angular frequency
- C is the capacitance of the circuit
- L is the inductance of the circuit

We can solve for C as follows:

$$\frac{1}{\omega C} = \omega L \tag{32}$$

$$1 = \omega^2 LC \tag{33}$$

$$C = \frac{1}{\omega^2 L} \tag{34}$$

We can determine the C required to amplify a given Larmor precession frequency by substituting in the precession frequency $f = \omega/2\pi$:

$$C = \frac{1}{(2\pi f)^2 L} = \frac{1}{4\pi^2 f^2 L} \tag{35}$$

The NMR apparatus allows a user to configure its capacitance to amplify certain frequencies as described here. This amplification makes it much more feasible to record the behavior of the emf output by the coil, and to isolate behavior related to Larmor precession specifically.

B Uncertainty Analysis

B.1 Spin-Lattice Relaxation Time

The recorded voltages V have uncertainty σ_V due to the limited precision of the oscilloscope. We quantified this uncertainty by taking several V measurements at the same polarization time, calculating a standard deviation of these measurements, and dividing by the mean measurement to get a percent error. This procedure gave $\sigma_V = 5.9\%$ for the free precession signal and $\sigma_V = 2.6\%$ for the NMR amplitude signal. Selected polarization times t_p are estimated as having a maximum uncertainty of $\sigma_{t_p} = 0.05\,\text{s}$, which is half value of the least significant digit that can be selected with the apparatus.

An initial unweighted fit was performed for both the free precession and NMR amplitude signals using Eq. 7. A weighted fit was then performed using a total uncertainty σ_{tot}:

$$\sigma_{tot} = \sqrt{\sigma_V^2 + \sigma_{t_p}^2 \left(\frac{V_0}{T_1} e^{-t_p/T_1}\right)^2} \tag{36}$$

which generated the fits shown in Figure 3.

The residuals for Figure 3 are shown in Figure 7. None of the residuals demonstrate a clear pattern, and all of the residual values lie close to zero. This indicates that Eq. 7 accurately models the behavior of the collected data.

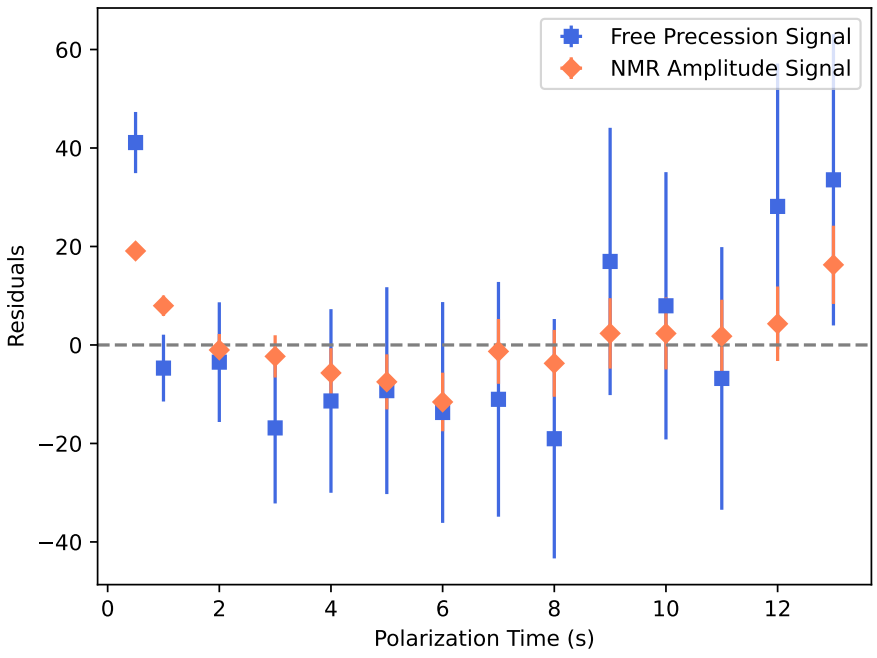

Figure 7: This plot displays the residuals of the polarization time versus voltage data. The residuals show no clear pattern and lie close to zero, indicating that the implemented exponential fit accurately models this dataset.

B.2 Curie Law

The recorded voltages V have uncertainties $\sigma_V = 5.9\%$ for the free precession signal and $\sigma_V = 2.6\%$ for the NMR amplitude signal, as described above. Selected sample coil currents I have uncertainty $\sigma_I = 0.15\% + 5\,\text{mA}$ as given in the power supply's manual [8].

An initial unweighted fit was performed for both the free precession and NMR amplitude signals using Eq. 9. Note that a y-intercept parameter b is included here to account for the sample having a non-zero magnetization at zero sample coil current due to the Earth's magnetic field. Since we only aim to verify a linear relationship between V and I, the magnitude of these fitting parameters is not relevant to verifying the form of the Curie law. A weighted fit was then performed using a total uncertainty σ_{tot}:

$$\sigma_{tot} = \sqrt{\sigma_V^2 + \sigma_I^2 \cdot m^2} \tag{37}$$

which generated the fits shown in Figure 4.

The residuals for Figure 4 are shown in Figure 8. None of the residuals demonstrate a clear pattern, and all of the residual values lie close to zero. This indicates that Eq. 9 accurately models the behavior of the collected data.

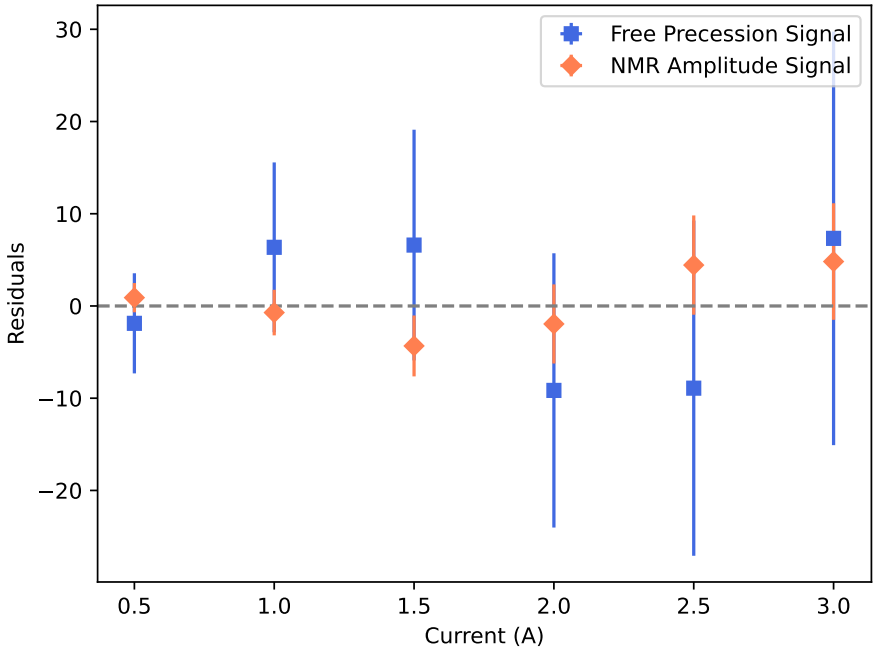

Figure 8: This plot displays the residuals of the polarization current versus voltage data. The residuals show no clear pattern and lie close to zero, indicating that the implemented linear fit accurately models this dataset.

B.3 Gyromagnetic Ratios

The recorded frequencies f are measured using the oscilloscope's frequency detection functionality, and therefore have uncertainty σ_f due to the limited precision of the oscilloscope. This uncertainty was quantified using the same technique as σ_V in Appendix B.1. This procedure gave $\sigma_f = 0.39\%$. Selected Helmholtz coil currents I_H are measured using a multimeter and have uncertainty $\sigma_{I_H} = 0.1\% + 3\,\text{mA}$ as given in the multimeter's manual [9].

An initial unweighted fit was performed using Eq. 10. A weighted fit was then performed using a total uncertainty σ_{tot}:

$$\sigma_{tot} = \sqrt{(\sigma_f)^2 + (\sigma_{I_H} \cdot m)^2} \tag{38}$$

A gyromagnetic ratio γ and estimation for Earth's magnetic field strength $B_\oplus$ can then be determined for each sample using Eq. 11. The error on calculated gyromagnetic ratios σ_γ is

$$\sigma_\gamma = \sqrt{\left(\frac{2\pi \cdot \sigma_m}{k}\right)^2 + \left(\frac{2\pi \cdot m \cdot \sigma_k}{k^2}\right)^2} \tag{39}$$

The error on estimations of Earth's magnetic field strength $\sigma_{B_\oplus}$ is

$$\sigma_{B_\oplus} = \sqrt{\left(\frac{2\pi \cdot \sigma_b}{\gamma}\right)^2 + \left(\frac{2\pi \cdot b \cdot \sigma_\gamma}{\gamma^2}\right)^2} \tag{40}$$

The error σ_k on the proportionality constant k from Eq. 28 is derived from errors on the measurement of the radius σ_R. We estimate $\sigma_r = 0.5\,\text{cm}$ based on the acuity of the human eye and the markings of the meter-stick used to measure the Helmholtz coil diameter. σ_k is then as follows:

$$\sigma_k = \frac{N\mu}{R^2} \cdot \sigma_R \tag{41}$$

The residuals for Figures 5 and 6 are shown in Figures 9 and 10 respectively. None of the residuals demonstrate a clear pattern, and all of the residual values lie close to zero. This indicates that Eq. 10 accurately models the behavior of the collected data.

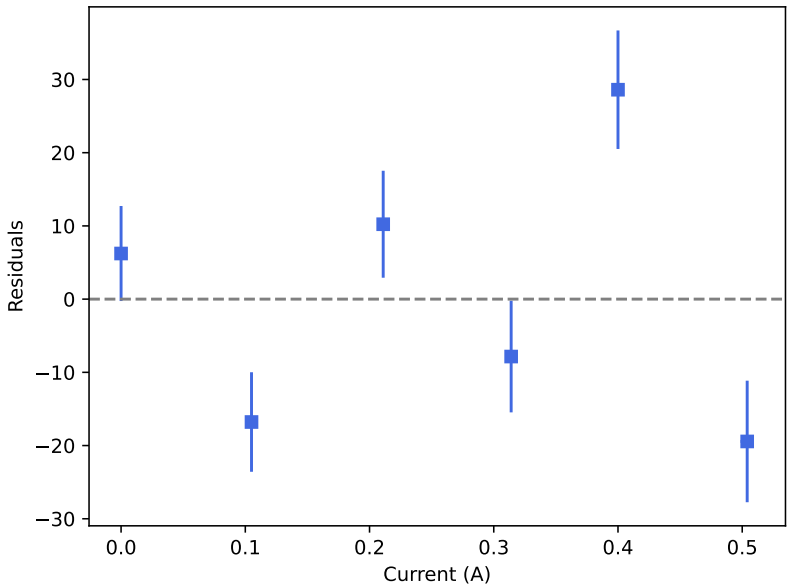

Figure 9: This plot displays the residuals of the Helmholtz coil current versus signal frequency data for tap water. The residuals show no clear pattern and lie close to zero, indicating that the implemented linear fit accurately models this dataset.

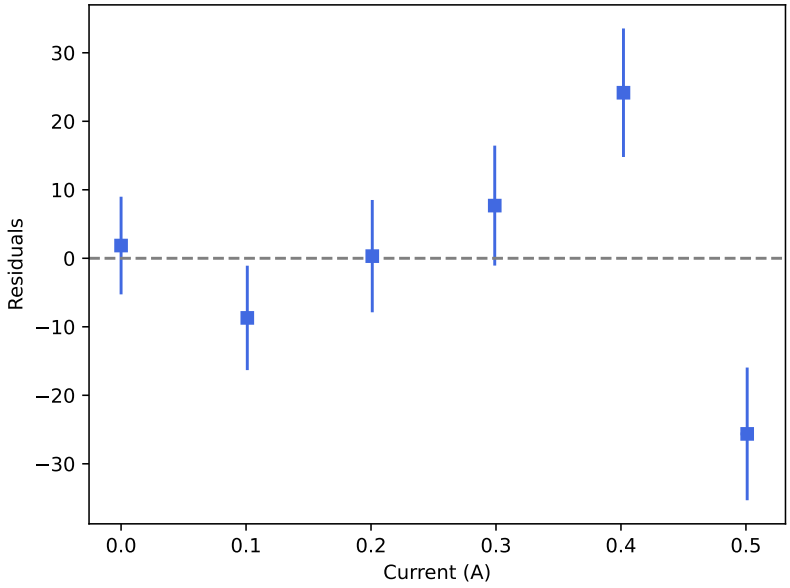

Figure 10: This plot displays the residuals of the Helmholtz coil current versus signal frequency data for the liquid fluorine compound. The residuals show no clear pattern and lie close to zero, indicating that the implemented linear fit accurately models this dataset.

C Gradient Field Coil Tuning

Our data was substantially impacted by issues tuning the gradient field coils on the apparatus.

The gradient field coils are designed to minimize the inhomogeneities in the Earth's magnetic field passing over the sample. These coils must be re-tuned throughout the experiment as the sample, apparatus settings, and Earth's magnetic field change. Throughout our experiment, we continually faced difficulties in getting the gradient field coils to properly homogenize external magnetic fields, and in some cases were unable to find any settings that provided consistent data to analyze. This impacted the quality of data for spin-lattice relaxation times, gyromagnetic ratio calculations, and especially spin-spin relaxation times.

C.1 Spin-Spin Relaxation Time

Due the the above issue, our collected spin-spin relaxation time T_2^* data was not usable for fitting. The free precession signal consistently decayed before reaching the oscilloscope's trigger point. An attempt to fit Eq. 8 gave $T_2^* \approx 10^6\,\text{s}$, which is several orders of magnitude larger than the expected $T_2^* \approx 2.5\,\text{s}$ [4]. Figure 11 presents an example of a T_2^* signal decaying before reaching the oscilloscope's trigger.

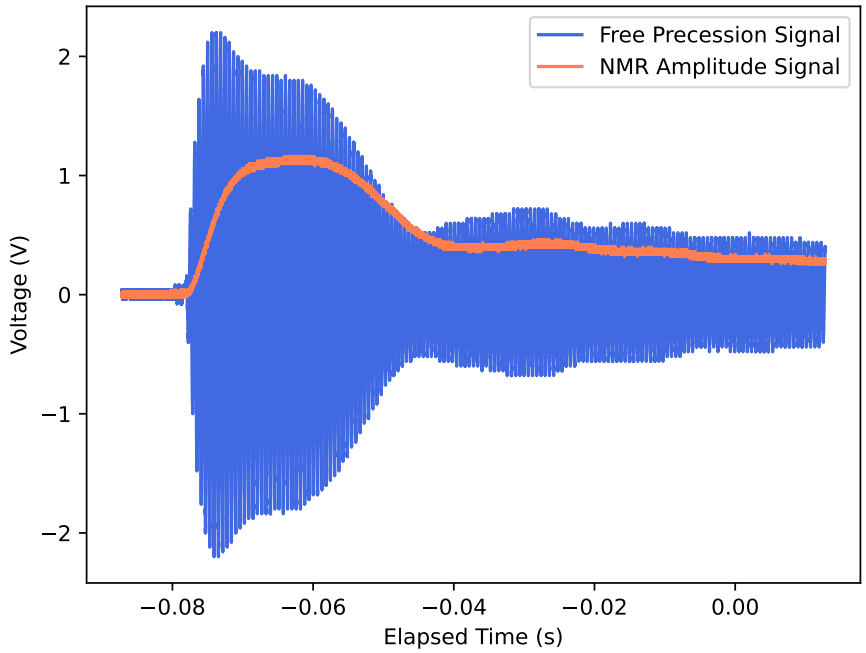

Figure 11: This plot displays the free precession and NMR amplitude voltage signals as a function of time for a tap water sample. The signal decays before reaching the trigger point at $t = 0\,\text{s}$, meaning the data is not usable for fitting.

References

[1] Peter A. Rinck. Non-medical applications of nmr and mri - magnetic resonance in medicine – the basics. https://www.magnetic-resonance.org/ch/19-01.html, 2024.

[2] Bill Melton. *Student Manual #2: Advanced Topics in Earth's-Field NMR*. TeachSpin, Inc., 2025. Covers gyromagnetic ratio, Curie law, and relaxation times.

[3] Charles Kittel. *Introduction to Solid State Physics*. Wiley, Hoboken, NJ, global edition, [9th edition] edition, 2018.

[4] Bill Melton. *Student Manual #1: Nuclear Magnetic Resonance in the Earth's Magnetic Field*. TeachSpin, Inc., 2025. Instruction manual for Earth's-field NMR experiments.

[5] *READ ME: Earth's Field Nuclear Magnetic Resonance (EFNMR) Experiment*. Carmen/Canvas, 2024.

[6] Donald H. Perkins. *Introduction to High Energy Physics*. Addison-Wesley, London, 2. ed., rev.enl.reset, 2. print edition, 1983.

[7] Wolfgang Pauli. Exclusion principle and quantum mechanics discours prononcéà la réception du prix nobel de physique 1945. *Dialectica*, 1(2):204–204, May 1947.

[8] Keysight e363xa series programmable dc power supplies datasheet. https://www.keysight.com/us/en/assets/7018-06785/data-sheets/5968-9726.pdf, 2025.

[9] Fluke 170 series true-rms digital multimeters. https://dam-assets.fluke.com/s3fs-public/6011663a-en-17x-ds-w_0.pdf?VersionId=e8AO6eNJpPsAUIhODD5LuxcacBfVJIy9, 2025.